Design of a Voltage Stabilized Power Supply Based on Back-Propagation Neural Network PID Control

1st Zhitong LI*
College of Physics and Information Engineering
Fuzhou University
Fuzhou, China
lizhitong1530@163.com*

2nd Yida ZHANG
Mathematics Department
King's College London
London, United Kingdom
z.yida@icloud.com

2nd Yuyao DENG
College of Physics and Information Engineering
Fuzhou University
Fuzhou, China
dyy021213@gmail.com

3rd Xin LI
R&D Department
Xiamen Taihang Technology Co., Ltd.
Xiamen, China
eocr@163.com

***Abstract*—To improve the dynamic response and steady-state accuracy of voltage-stabilized power supplies under complex conditions, this paper proposes a self-tuning PID control strategy using a neural network for AC voltage stabilization. Conventional PID controllers suffer from fixed parameters and slow adjustment, especially under large voltage fluctuations and frequent frequency changes, limiting their ability to meet modern power electronics' stringent requirements. To overcome these issues, a BP neural network is applied to dynamically optimize PID parameters online, harnessing its nonlinear fitting and adaptive capabilities. Simulations were carried out in Matlab/Simulink using a developed power supply model and neural network PID structure. Results show that the proposed system offers strong robustness, effectively suppresses voltage disturbances, and achieves low distortion, high precision, and fast response in the output voltage. Although output frequency is mainly governed by a phase-locked loop, the neural network PID enhances voltage waveform quality, stabilizing the fundamental frequency near the ideal 50 Hz. This work provides a viable approach toward intelligent control of traditional voltage-stabilized power supplies with high practical applicability.**

Keywords—Neural Network, PID Control, AC Voltage Regulator, PLL, Simulink Simulation

I. INTRODUCTION

In power electronics systems, PID controllers are widely used in the design and control of voltage-stabilized power supplies due to their simple structure, ease of implementation, and excellent steady-state and dynamic performance in linear systems [1-2]. However, when confronted with nonlinear dynamics, large time delays, parameter uncertainties, and external disturbances, traditional PID controllers often face challenges such as sluggish response, excessive overshoot, and insufficient robustness [3-4]. For instance, in a Buck-type DC-DC converter, the settling time of a conventional PID controller can reach up to 188 ms, with load and line regulation rates of 14.5% and 8.2%, respectively, while an improved control strategy achieves only 60 ms and 0.8%/0.33% [5]. These limitations not only restrict the overall system performance but may also lead to instability or inefficiency under complex operating conditions. Therefore, developing advanced adaptive control strategies to enhance dynamic response and robustness while ensuring system stability has become a research focus in the field of power electronics control.

In recent years, artificial neural networks (ANNs) have increasingly been integrated into control loops to provide online adaptation and nonlinear mapping capabilities. In particular, back-propagation (BP) neural networks can be trained to adjust PID gains in real time, enabling faster settling, better disturbance rejection, and lower harmonic content in regulated voltages [6].

Recent works have demonstrated the effectiveness of ANN-enhanced PID schemes for power-electronics regulation. For example, an adaptive PIDNN approach with hybrid metaheuristic initialization was shown to improve voltage regulation and harmonic performance for three-phase inverters in islanded microgrids [7]. Bio-inspired optimizers combined with BP neural networks have also been used to produce robust adaptive PID algorithms that improve transient response and convergence in converter control tasks [8]. Likewise, ANN-based architectures have been used to stabilize inverter/class-E outputs and to optimize inverter control under grid-connected conditions, indicating the broad applicability of neural PID ideas across converter topologies [9]. Motivated by these advances, this paper proposes a BP neural network–based self-tuning PID for an AC-DC-AC voltage-stabilized power supply. The BP network adapts K_P, K_I, and K_D online according to measured deviations, while an adaptive learning/weight-initialization mechanism enhances convergence and robustness. Simulation results (Matlab/Simulink) demonstrate faster settling, reduced frequency deviation, and improved waveform quality relative to a conventional fixed-gain PID baseline, showing the practical promise of BP-PID strategies in next-generation stabilized power supplies.

II. Working Principle

A. PID Controller

PID controllers are ubiquitous in industrial control applications. The traditional PID controller boasts a simple architecture, with its output mathematically represented by:

$$y(t) = K_P e(t) + K_I \int_0^t e(\tau)d\tau + K_D \frac{de(t)}{dt} \quad (1)$$

where, K_P, K_I, and K_D are termed the proportional, integral, and derivative gains, respectively. In a conventional PID controller, $e(t)$denotes the error signal, which is the deviation between the desired setpoint and the actual output value. The discretized form of the PID algorithm is given as follows:

$$u_k = K_P e(k) + K_I \sum e(k) + K_D[e(k) - e(k-1)]/T \quad (2)$$

where $e(k) = u(5) = y_{target} - y_{out} = R_{in} - V_{abc}$ is the current error between the desired and actual outputs. In this paper, the sampling time is set as $T = 0.001$ s. The three parameters of the PID controller are optimized through continuous adjustment of the weights between the hidden layer and output layer, as well as between the input layer and hidden layer of the BP neural network. Subsequently, the output u_k of the PID controller is computed and utilized to adjust the duty cycle of the PWM signal that drives the MOSFETs in the DC-AC module. By regulating the turn-on and turn-off times of the MOSFETs, the system achieves voltage stabilization.

B. Voltage Stabilized Power Supply System Based on BP Neural Network

This paper integrates a BP neural network with a discrete positional PID controller to realize a voltage-stabilized power supply system capable of dynamically adjusting PID parameters. This enables timely updates of the PID parameters to maintain voltage stabilization, even under wide variations in voltage and frequency. The system schematic is shown in Fig. 1. By setting the desired voltage reference R_{in}, the error signal $e(k)$ at this moment is obtained by taking the difference between R_{in} and the actual output voltage V_{abc}. This error signal $e(k)$, along with the desired voltage R_{in} and the current output voltage V_{abc}, are fed into the BP neural network. After optimization and adjustment of the weights, the network outputs the three parameters K_P, K_I, and K_D for the PID controller. The output of the PID controller u_k is then computed and sent to the PWM Generator to control the conduction time of the four IGBTs in the DC-AC section of the Converter. The Converter primarily consists of: an AC-DC stage, a DC-AC stage, and an RLC low-pass filter. The configured input voltage is supplied to the AC-DC module, then processed by the four PWM-controlled IGBTs in the DC-AC stage. Finally, the 50 Hz voltage signal is extracted through the low-pass filter. The AC-AC voltage-stabilized power supply adopted in this paper employs an indirect structure, namely AC-DC-AC. Additionally, all components in this study are ideal, disregarding practical non-idealities. As a result, the simulation outcomes align closely with theoretical expectations.

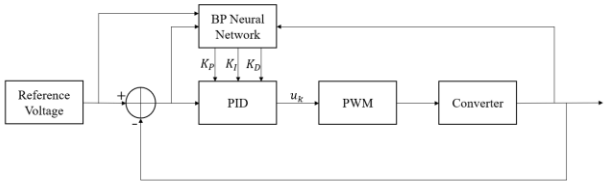

Fig. 1. Overall design of the BP-NN based PID voltage-stabilizing power supply system

C. BP Neural Network

The BP neural network achieves nonlinear mapping through its hierarchical structure, which consists of an input layer, hidden layer, and output layer. Its backpropagation algorithm dynamically adjusts the PID parameters—K_P, K_I, and K_D—to adapt to complex control scenarios. The BP neural network primarily employs the gradient descent method to minimize error. In this study, the input layer contains three nodes, which receive the following system signals: the reference voltage $u(1)$, the actual output voltage $u(3)$, and the deviation value $u(5)$ between them. The network structure is illustrated in Fig. 2. Here, x_1, x_2, and x_3 correspond to $u(1)$ (reference voltage), $u(3)$ (actual output voltage), and $u(5)$ (deviation), respectively. The outputs of the network are K_P, K_I, and K_D, which serve as the three parameters of the PID controller.

For each layer l in the network, a linear transformation is first applied to its input a : $z^{(l)} = w^{(l)}a^{(l-1)} + b^{(l)}$, Then, a nonlinear activation function is applied: $a^{(l)} = h(z^{(l)})$. Next, the input matrix of the network is constructed as follows:

$$x_i = [u(1), u(3), u(5)] \in \mathbb{R}^{H\times 3}$$

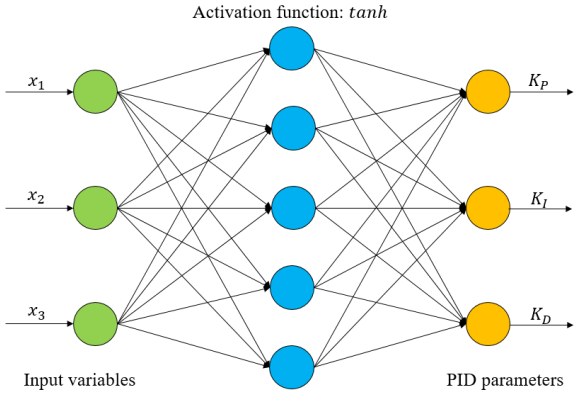

Fig. 2. Schematic Diagram of the BP Neural Network

The input to the hidden layer is:

$$I_l = x_i \cdot w_i^{\mathsf{T}}, \quad w_i \epsilon \mathbb{R}^{H\times 3}$$

Here, H denotes the number of nodes in the hidden layer. In this study, $H = 5$. The initial values of w_i are generated using the **rand(5,3)** function. The hyperbolic tangent function $tanh\ (x)$ is selected as the activation function for the hidden layer, and its output is given by:

$$O_l = \tanh\ (I_l)$$

The output of the hidden layer is multiplied by the weight matrix w_o to form the input to the output layer:

$$I_o = O_l \cdot w_O^{\top},\ \ w_o \epsilon \mathbb{R}^{3\times H}$$

Here, w_o is initialized using the **rand(3,5)** function. The output layer of the entire network employs a Sigmoid activation function, and the final outputs are the three parameters of the PID controller: K_P, K_I, and K_D. The weights of the network are updated via the error backpropagation algorithm. For the output layer weight adjustment, the direction of influence (positive/negative feedback) of the control variable change on the system output is calculated based on the system sensitivity:

$$dyu = sign\left(\frac{u(3)-u(2)}{u(7)-u(6)+\varepsilon}\right)$$

Here, $u(7)$ represents the current control output of the PID controller, while $u(6)$ denotes the control output from the previous time step. The term ε is a small constant introduced to prevent division by zero. Additionally, $u(3)$ corresponds to the actual output voltage at the current time step, and $u(2)$ indicates the actual output voltage from the previous time step. The primary purpose of this sign function is to determine the instantaneous response direction of the system by calculating the ratio between the change in the output voltage of the regulated power supply and the change in the control output of the PID controller. By leveraging the sign of dyu, the propagation direction of the error is adjusted, ensuring that the weight updates align with the dynamic characteristics of the actual system.

The experiment employs the mean squared error (MSE) as the objective function:

$$L = \frac{1}{2}\left(y_{target} - y_{out}\right)^2 \tag{3}$$

The error term formula for the output of the l-th layer in the BP neural network is defined as:

$$\delta^{(l)} = \frac{\partial L}{\partial z^{(l)}}$$

Specifically, for the final output layer, we have:

$$\delta^{(L)} = \frac{\partial L}{\partial O^L} = \frac{\partial L}{\partial y_{target}}\ \frac{\partial y_{target}}{\partial O^L} = (y_{target} - y_{out}) \cdot g'(z)$$

where $g'(z)$ is the derivative of the output layer activation function. In this paper, $y_{target} - y_{out}$ corresponds to the control error signal $u(5)$ defined herein. The error gradient is adjusted by incorporating the system dynamic direction dyu and the PID component $epid(i)$. In the S-function, the error gradients for K_P, K_I, and K_D are respectively defined as:

$$\delta^{(L)}(1) = u(5) \cdot dyu \cdot e(t) dk(1)$$

$$\delta^{(L)}(2) = u(5) \cdot dyu \cdot \sum e(t)\, dk(2)$$

$$\delta^{(L)}(3) = u(5) \cdot dyu \cdot \Delta e(t) dk(3)$$

where $dk(i)$ represents the derivative of the activation function corresponding to the i-th PID coefficient. From $z^{(l+1)} = w^{(l+1)}a^{(l)} + b^{(l+1)}$, the element-wise derivative of the matrix $a^{(l)}$ is computed, and applying the chain rule yields:

$$\frac{\partial L}{\partial a_{ij}^{(l)}} = \sum_{p=1}^{m}\sum_{q=1}^{n} \frac{\partial L}{\partial z_{pq}^{(l+1)}} \cdot \frac{\partial z_{pq}^{(l+1)}}{a_{ij}^{(l)}} \sum_{p=1}^{m} \frac{\partial L}{\partial z_{pj}^{(l+1)}} \cdot \frac{\partial z_{pj}^{(l+1)}}{a_{ij}^{(l)}} = \sum_{p=1}^{m} w_{pi}^{(l+1)} \cdot \frac{\partial L}{\partial z_{pj}^{(l+1)}}$$

Observing the structure of the above expression, it can be noted that the matrix form is equivalent to:

$$\frac{\partial L}{\partial a^{(l)}} = (w^{(l+1)})^{\top} \cdot \frac{\partial L}{\partial z^{(l+1)}} = (w^{(l+1)})^{\top} \cdot \delta^{(l+1)}$$

Therefore, given the error term of the $(l+1)$-th layer, the error term of the l-th layer can be recursively derived, and this term can be solved via the chain rule to establish its recurrence relation:

$$\delta^{(l)} = \frac{\partial L}{\partial z^{(l)}} = \left(\frac{\partial L}{\partial a^{(l)}} \cdot \frac{\partial a^{(l)}}{\partial z^{(l+1)}}\right) \odot f'\left(z^{(l)}\right) = \left((w^{(l+1)})^{\top} \cdot \delta^{(l+1)}\right) \odot f'\left(z^{(l)}\right)$$

It follows that the error gradient expression is given by:

$$\nabla w^{(l)} = \frac{\partial L}{\partial w^{(l)}} = \frac{\partial L}{\partial z^{(l)}} \cdot \frac{\partial z^{(l)}}{\partial w^{(l)}} = \delta^{(l)} \cdot \left(a^{(l-1)}\right)^{\top}$$

$$\nabla \mathrm{b}^{(l)} = \delta^{(l)}$$

After computing the error gradient, the weight adjustments for the output layer of each layer are calculated. The weight adjustments are determined using the gradient descent method combined with a momentum term:

$$\Delta w^{(l)}(t) = \eta \cdot \nabla w^{(l)}(t)\ \ + \alpha \cdot \Delta w^{(l)}(t-1) = \eta \cdot \delta^{(l)}(t) \cdot (O^{(l)})^{\top}\ \ + \alpha \cdot \Delta w^{(l)}(t-1) \tag{4}$$

$$\Delta b^{(l)}(t) = \eta \cdot \nabla \mathrm{b}^{(l)}(t) + \alpha \cdot \Delta b^{(l)}(t-1) = \eta \cdot \delta^{(l)}(t) + \alpha \cdot \Delta b^{(l)}(t-1) \tag{5}$$

where η is the learning rate, used to mitigate the risk of overfitting during neural network optimization; α is the momentum coefficient, which incorporates the previous update to stabilize the optimization direction and accelerate convergence; and t denotes the number of iteration cycles, representing the t-th iteration at this moment.

After obtaining Δw_o, it is added to the original output layer weights to obtain the updated weights. The weight adjustments for the hidden layer follow the same principle, with their gradients computed via the chain rule during backpropagation. The core formula used in gradient descent is:

$$w^{(l)}(t+1) \leftarrow w^{(l)} - \Delta w^{(l)}(t) \tag{6}$$

$$b^{(l)}(t+1) \leftarrow b^{(l)} - \Delta b^{(l)}(t) \tag{7}$$

Through repeated iterations, the weight matrix gradually converges from its initial random values to a local minimum of the loss function.

III. Simulation and Results Analysis

This paper constructs a simulation circuit using the Simulink functionality in Matlab. The simulation circuit of the BP neural network-controlled PID voltage-stabilized power supply is shown in Fig. 3. Furthermore, by comparing the output of the BP neural network-controlled PID voltage-stabilized power supply with that of a conventional voltage-stabilized power supply, the improvement offered by the neural network-based approach is validated.

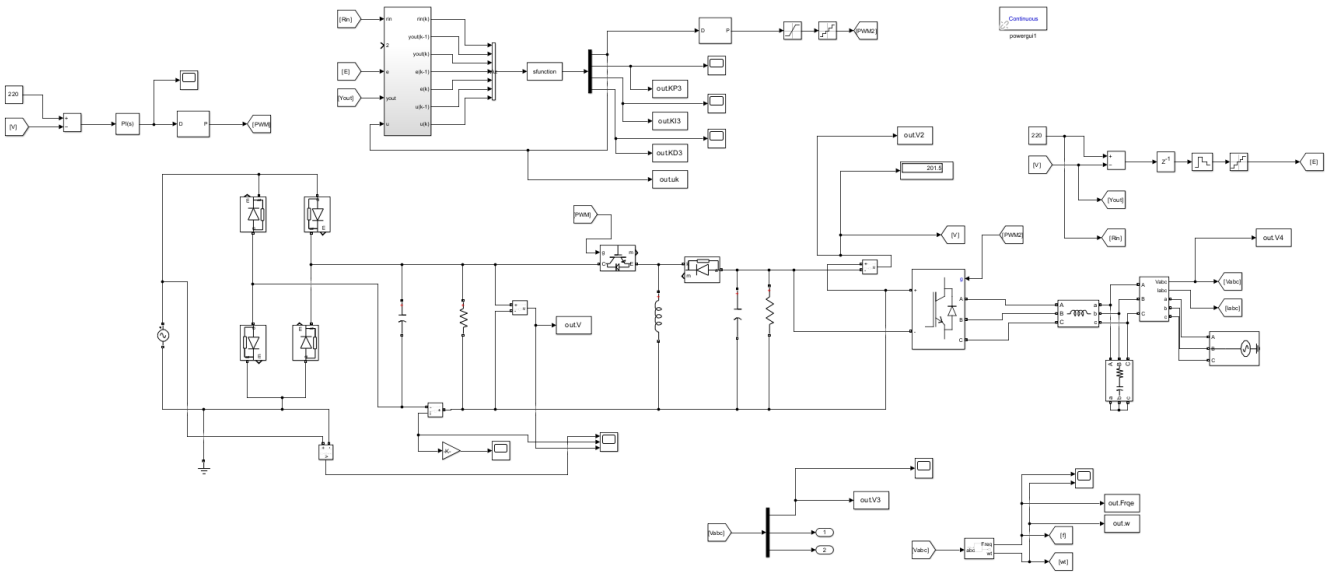

Fig.3. Simulation Circuit Diagram of the BP Neural Network-Controlled PID Voltage-Stabilized Power Supply.

A total of four sets of data with different input voltages and frequencies were tested. By comparing the performance of the conventional PID voltage-stabilized power supply and the BP neural network-based PID voltage-stabilized power supply in terms of settling time, waveform frequency components, overshoot, and steady-state amplitude, the effectiveness of the proposed method is validated. It should be noted that non-ideal factors such as device losses, switching delays, and noise were neglected during the simulation in this study.

The experimental data of the BP neural network-controlled PID voltage-stabilized power supply are presented in Table 1. The data in Table 1 demonstrate that, under identical conditions, the BP neural network-controlled PID voltage-stabilized power supply achieves a significantly reduced settling time, with an average settling time of approximately 5 ms. This indicates that the BP neural network can rapidly adjust PID parameters, enabling the system to reach a stable state more quickly. Under the same input conditions, the output peak voltage of the BP neural network-controlled PID voltage-stabilized power supply is 220.4 V, and the trough voltage is -220.4 V, which are nearly identical to the set value. This result confirms that the BP neural network-controlled PID voltage-stabilized power supply exhibits superior output voltage stability and enhanced capability to suppress input disturbances.

Table 1. Experimental Data of the BP Neural Network-Controlled PID Voltage-Stabilized Power Supply.

Input Setting	Settling Time (ms)	Stable Peak Voltage (V)	Stable Trough Voltage (V)	Stable Frequency (Hz)
220V 50Hz	5.021	220.3	-220.5	50.209
200V 48Hz	5.076	220.4	-220.4	49.586
230V 52Hz	5.073	220.4	-220.4	49.931
240V 55Hz	5.076	220.4	-220.4	49.586

When the input is set to 220 V and 50 Hz, the time-domain waveforms and amplitude-frequency characteristics of the output from both the proposed BP neural network-controlled PID voltage-stabilized power supply system and the conventional PID-based system are shown in Fig.4 and Fig. 5, respectively.

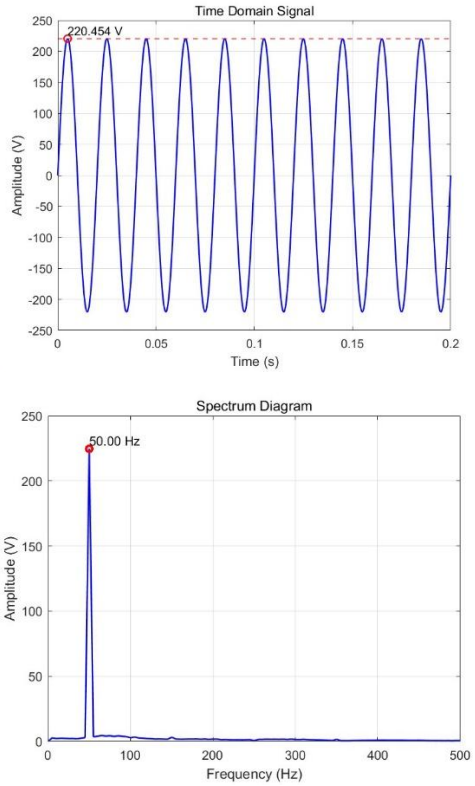

Fig. 4. Time-domain waveform and amplitude-frequency characteristic curve of the output when the input is set to 220 V and 50 Hz.

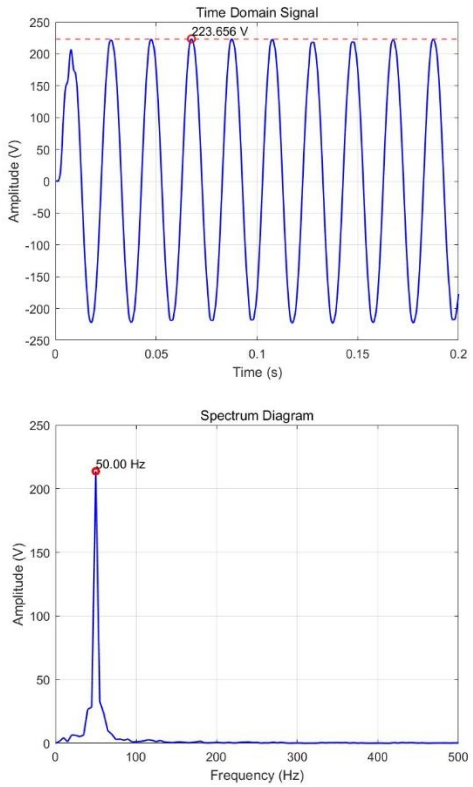

Fig. 5. Time-Domain Waveform and Amplitude-Frequency Characteristic Curves of the Output at 220 V, 50 Hz Input Setting.

The output behaviors of the two systems under other input settings are similar, and their specific time-domain waveforms and frequency spectra are not shown here for brevity. In the conventional PID-controlled voltage-stabilized power supply, significant fluctuations occur in the peak and trough values of the output voltage when the input voltage and frequency vary. For example, with an input of 220 V / 48 Hz, the output peak reaches 223.656 V, while the trough measures –206.5 V. In this study, the output frequency is determined by a phase-locked loop (PLL). Thus, theoretically, the output frequency should remain around 50 Hz and not change significantly with fluctuations in the grid frequency. However, in the conventional PID-controlled system, due to fixed control parameters, dynamic regulation of the output inverter bridge is insufficient when the input frequency deviates from 50 Hz. This may lead to distorted voltage waveforms, manifesting as deviation of the fundamental frequency component or the presence of strong harmonic components in the frequency spectrum. For instance, with an input of 240 V / 55 Hz, the dominant output frequency approaches 55 Hz, indicating inadequate filtering and control precision. In contrast, the BP neural network-based PID controller adapts its parameters online according to the dynamic characteristics of the system, enabling more precise voltage regulation and suppressing frequency deviation caused by waveform distortion. Under the same input conditions, the fundamental frequency of the output remains consistently around 50 Hz (e.g., within 49.6–50.2 Hz), aligning with the system reference frequency. This indicates that the neural network-enhanced PID primarily improves the quality of the voltage waveform, thereby indirectly enhancing the stability of the frequency components.

The frequency spectra obtained via Fast Fourier Transform (FFT) reveal that the output waveform of the conventional PID-controlled power supply contains noticeable high-frequency components, with significant distortion observed in the time domain. In contrast, the output waveform of the BP neural network-controlled PID system more closely resembles an ideal sine wave, exhibiting fewer high-frequency components and superior waveform quality. This further demonstrates the advantage of the BP neural network-based PID control in suppressing high-frequency disturbances.

The variations of the three parameters (K_P, K_I, K_D) of the BP neural network-based PID controller are shown sequentially from top to bottom in Fig. 6. As can be observed from the figure, the values of K_P, K_I, and K_D are automatically adjusted under different input conditions to adapt to dynamic changes in the system. This self-adaptive capability, which is absent in conventional PID controllers, is one of the key factors contributing to the superior performance of the BP neural network-controlled PID voltage-stabilized power supply.

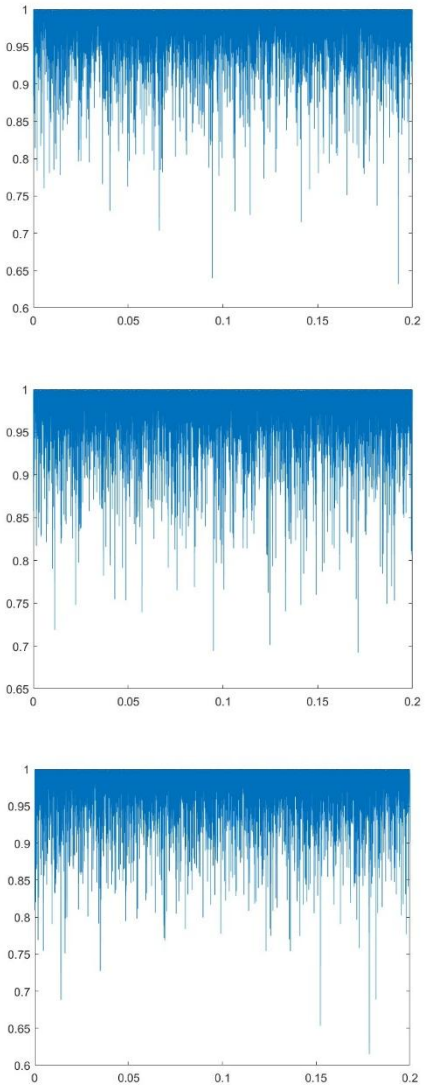

Fig. 6. Variation curves of K_P, K_I, and K_D when the input is set to 220 V and 50 Hz

IV. Conclusion

This paper addresses the common issues of slow dynamic response and large steady-state error in conventional PID voltage-stabilized power supplies under wide-range disturbances in input voltage and frequency. A self-tuning PID control strategy based on a BP neural network is proposed and validated. A simulation model was built using Matlab/Simulink, and comparative experiments with a conventional PID controller were conducted under five typical operating conditions. The main conclusions are as follows:

(1) The BP neural network PID control greatly reduces the average settling time, which significantly accelerates the system's dynamic response.

(2) The voltage deviation under various operating conditions, significantly outperforms conventional PID control, as demonstrates its effective suppression of input disturbances.

(3) The BP neural network-based PID control reduces the maximum deviation between the output frequency and the set value, as greatly improves system frequency stability.

(4) The output waveform under BP neural network-based PID control contains lower higher-harmonic content and more closely approximates an ideal sine wave.

(5) BP neural network can adjust K_P, K_I, and K_D online in response to input disturbances, enabling adaptive optimization of the controller and validating the effectiveness of the designed system.

Although the proposed method achieves favorable results in the simulation environment, certain limitations and areas for improvement remain. For instance, the simulation model does not account for practical factors such as power device nonlinearities, measurement noise, or abrupt load changes. Future work could include experimental validation using physical hardware to further verify the engineering practicality of the algorithm. Additionally, the training of the BP neural network relies on initial weights and is prone to becoming trapped in local minima.

References

[1] Johnson M A, Moradi M H. PID control[M]. London, UK: Springer-Verlag London Limited, 2005.

[2] Hu, B., Long, S., Jiang, G., et al. Research on Loop Compensation of Buck Switching Power Supply Based on PID Algorithm. Industrial Control Computer, 2024, 37(06): 152-154.

[3] Chauhan R K, Rajpurohit B S, Hebner R E, et al. Design and analysis of PID and fuzzy-PID controller for voltage control of DC microgrid[C]//2015 IEEE Innovative Smart Grid Technologies-Asia (ISGT ASIA). IEEE, 2015: 1-6.

[4] Zhao, C., & Guo, L. (2019). Extended PID control of nonlinear uncertain systems. arXiv preprint arXiv:1901.00973.

[5] Ma, B.; Jiao, J.; Ye, Z. Adaptive Fast Integral Terminal Sliding Mode Control Strategy Based on Four-Switch Buck–Boost Converters. *Energies* 2024, *17*, 3645. https://doi.org/10.3390/en17153645

[6] M. M. Hasan, M. S. Rana, F. Tabassum, H. R. Pota, and M. H. K. Roni, "Optimizing the initial weights of a PID neural network controller for voltage stabilization of microgrids using a PEO-GA algorithm," Appl. Soft Comput., vol. 147, Art. no. 110771, 2023. doi:10.1016/j.asoc.2023.110771

[7] W. Kong, H. Zhang, X. Yang, Z. Yao, R. Wang, W. Yang, and J. Zhang, "PID control algorithm based on multistrategy enhanced dung beetle optimizer and back-propagation neural network for DC motor control," Sci. Rep., vol. 14, Art. no. 28276, Nov. 2024. doi:10.1038/s41598-024-79653-z

[8] M. Khodadoost, M. Hayati, and H. Abbasi, "Design of a class E inverter with stabilized output power using dual artificial neural networks for applications in biomedical implants," Sci. Rep., vol. 15, Art. no. 31158, 2025. doi:10.1038/s41598-025-15990-x

[9] M. Gupta, P. M. Tiwari, R. K. Viral, A. Shrivastava, B. A. Zneid, and I. Hunko, "Grid-connected PV inverter system control optimization using Grey Wolf optimized PID controller," Sci. Rep., vol. 15, Art. no. 28869, 2025. doi:10.1038/s41598-025-10617-7